Improved State Estimation Using Lagrange Relaxation to Include Operating Limits of VSC-MTDC System

Wei Feng, Qingxin Shi, Hantao Cui, Fangxing Li
Department of Electrical Engineering & Computer Science
The University of Tennessee, Knoxville
Knoxville, USA

Chen Yuan, Renchang Dai, Guangyi Liu
GEIRI North America Inc
Santa Clara, USA

***Abstract*—This paper proposes an improved state estimation (SE) method by combining Lagrange relaxation with the conventional WLS (weighted least square), to include the operating limits of VSC-MTDC (voltage sourced converter, multi-terminal direct current) system. Taking advantage of the fast-regulating ability of PWM (pulse-width modulation) used in VSC, the operating range of the converter is strictly restricted within the limits. And, when the limits are violated, the corresponding change in control strategy can be done in a very short time. Therefore, SE should reflect the violations give the accurate limit values. However, the conventional SE approaches, which rely on global optimal solutions, may fail to deal with the operating limits due to the measurement errors. To improve, three contributions are made in this paper. First, the operating limits together with the regulations are analyzed in detail. Then, a procedure of violations check is implemented inside the Sequential Method. Finally, once the violated estimations are detected, the corresponding equality constraints which represent the adjustments are added on the WLS functions, and solved by using Lagrange relaxation. The accuracy and efficiency of the proposed method is tested on two typical systems with different control parameters.**

***Index Terms*—Lagrange relaxation, MTDC, Operating limits, State estimation, VSC.**

I. Introduction

With the growing need for modern power systems operating with larger capacity, longer transmission distance and higher reliability, the HVDC (high voltage direct current) projects have drawn great attention worldwide [1]-[2]. Besides the outstanding features mentioned above, one of the advantages of VSC technology over the traditional LCC (line-commutated converter) technology is the ability of connecting multiple asynchronous AC grids to compose a larger system with multi-terminal links. Thus, various renewable energy sources can be integrated in one system. In recent years, more VSC-MTDC systems have been established or planned [3]-[4].

However, some research issues come together with the technical advantages. One issue is the state estimation (SE), which is one of the most important functions in EMS (energy management system). The extra complexities in modeling the topology and steady-state operations of VSC-MTDC systems bring great challenges to SE. In order to monitor the hybrid systems, some SE methods have been proposed. Generally, they can be classified into the Unified Method [5] and the Sequential Method [6]. In the Unified Method, all the measurements, state variables and operating functions of both AC and DC grids are formulated as a single integrated problem and solved by generating a modified matrix of WLS algorithm. However, since this approach requires modifying the existing SE software for AC networks, all the SE needs reprogramming. Furthermore, it is hard for us to control the internal behaviors of VSC independently without affecting the entire solver. In the Sequential Method, on the contrary, there are two calculating loops for sequential SE. The AC and DC grids are solved separately in the inner loops, and then the global convergence check is performed in the outer loops. Thus, it has the major advantage of being easily implemented as an extended function to the mature SE software for AC networks. Furthermore, as discussed in [7], the converter measurements are allowed to be updated and replaced easily in the Sequential Method. A generalized SE model for VSC was proposed in [8], and a distributed approach which can do SE in a decentralized calculation was given in [9].

However, another important feature of VSC is still not fully explored in the SE analysis. Compared with the generators and motors, which are hard to be controlled accurately in a short time due to the large rotational inertia, VSC can self-adjust the operating status quickly by PMW control. Therefore, under normal conditions, the true operating values of VSC should always be within the safe range or on the boundaries. Hence, SE should monitor violations and provide accurate values if needed. Whereas, the estimations of the conventional WLS algorithm may exceed the range and fail to represent the accurate limit values because of the drawback of global optimization on all measurement errors.

There are three main contributions in this paper. First, the VSC-MTDC system is modeled in detail for analyzing the operating limits. Furthermore, the adjustments on the corresponding violations are illustrated. Second, a procedure of violations check is added to improve the Sequential Method. Finally, once violations are detected, the corresponding equality constraints will be added to the WLS

This work is supported by the State Grid Corporation technology project 5455HJ180020.

equations, and solved by introducing Lagrange relaxation. Consequently, the improved SE method considers the operating limits with high accuracy.

The paper is organized as follows. Section II briefly describes the SE model of VSC-MTDC system together with WLS algorithm. Section III analyzes the operating limits and the corresponding adjustments of VSC. Section IV presents the improved SE method together with the Lagrange relaxation method. Section V illustrates the accuracy and efficiency of the proposed method by case studies.

II. SE Model of VSC-MTDC System

A. *Steady-state operation of VSC-MTDC system*

In the most general and simple format, the modeling of steady-state power flow model of VSC-MTDC system is shown in Fig. 1.

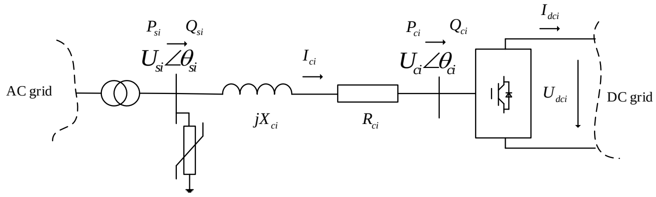

Figure 1. Single phase model of a typical VSC-MTDC system

A typical VSC-MTDC system can be naturally decoupled into three sub-regions, a.k.a., the AC grid, the DC grid and the converter. Thus, the steady-state operation of each part can also be analyzed individually.

1) AC grid. as the main component of the entire system, most of the AC buses and lines can be modeled as pure AC network. Thus, the equations representing power balance can be modeled as:

$$P_{aci} = U_{aci} \sum_{j\in i} U_{acj} (G_{acij} \cos\theta_{acij} + B_{acij} \sin\theta_{acij}) \quad (1)$$

$$Q_{aci} = U_{aci} \sum_{j\in i} U_{acj} (G_{acij} \sin\theta_{acij} - B_{acij} \cos\theta_{acij}) \quad (2)$$

where G_{acij} and B_{acij} are the real and imaginary parts of the admittance. For the power balance on PCC, the power injection can be modeled as an extra load on the corresponding buses. Thus, P_{si} and P_{ci} are added to (1) and (2), respectively.

2) DC grid. Without the line reactance and voltage angle, a DC grid can be modeled based on the voltage and current easily as:

$$I_{dci} = \sum_{j=1, j\neq i}^{n} Y_{dci,j} (U_{dci} - U_{dcj}) \quad (3)$$

Furthermore, the power injection to the DC bus can be calculated as:

$$P_{dci} = U_{dci} I_{dci} = U_{dci} \sum_{j=1, j\neq i}^{n} Y_{dci,j} (U_{dci} - U_{dcj}) \quad (4)$$

Since the power injection from converter to DC bus is active power, the power balance should be $P_{ci} = P_{dci}$.

3) Converter. Converter is the core device in the VSC-MTDC system. Since the behaviors of inverters and rectifiers are similar, the rectifier is modeled here to simplify the analysis in Fig. 1. First, the converter current can be solved as:

$$I_{ci} = (U_{si} - U_{ci}) / (R_{ci} + jX_{ci}) \quad (5)$$

Then, the power injection to both AC and DC grids can be calculated from $S_{si} = U_{si} I_{ci}^*$ and $S_{ci} = U_{ci} I_{ci}^*$. To slimily the equations, let $\delta_i = \theta_{si} - \theta_{ci}$, $\alpha_i = tan^{-1}(R_{ci}/X_{ci})$ and $Y_i = 1/\sqrt{R_{cii}^2 + X_{ci}^2}$. Then, the power injections are given by:

$$P_{si} = U_{si} U_{ci} Y_i \sin(\delta_i - \alpha_i) + U_{si}^2 Y_i \sin\alpha_i \quad (6)$$

$$Q_{si} = -U_{si} U_{ci} Y_i \cos(\delta_i - \alpha_i) + U_{si}^2 Y_i \cos\alpha_i \quad (7)$$

$$P_{ci} = U_{si} U_{ci} Y_i \sin(\delta_i + \alpha_i) - U_{ci}^2 Y_i \sin\alpha_i \quad (8)$$

$$Q_{ci} = U_{si} U_{ci} Y_i \cos(\delta_i - \alpha_i) - U_{ci}^2 Y_i \cos\alpha_i \quad (9)$$

Also, it should be noted that the voltage U_{ci} and U_{si} is determined by the input from the corresponding AC and DC buses, and can be given as:

$$U_{si} = U_{aci} / T_{si} \quad (10)$$

$$U_{ci} = \mu_i M_i U_{dci} / \sqrt{2} \quad (11)$$

Hence, equations (1)-(11) form the basic steady-state model of VSC-MTDC system. Furthermore, as a fully-controllable device, each VSC can be preset with constant target values. In a multi-terminal link, one DC bus operates as the slack bus with reference value to regulate power balance. Then, other converters are controlled to provide constant power injections. Normally, these preset values of control strategy can be regarded as high-weighted pseudo-measurements.

B. *WLS algorithm*

The steady-state SE is a process of obtaining accurate estimation of state variables from noisy, uncertain but redundant measurements. In general, the relationships between measurements and state variables is given by

$$z = h(x) + e \quad (12)$$

where *z*, *h*, *x* and *e* are the sets of measurements, operating functions, state variables and errors respectively. To solve (12), the extensively used method is WLS, which is utilized to minimize the following objective function:

$$J(x) = [z - h(x)]^T W [z - h(x)] \quad (13)$$

where *W* is the matrix of weights. According to the first-order optimality conditions, the approximate solution can be obtained by solving the following equation iteratively:

$$G(x^k)\Delta x^k = H(x^k)^T W [z - h(x)] \quad (14)$$

$$x^{k+1} = x^k + \Delta x^k \quad (15)$$

In general, WLS is always solvable with enough redundant measurements. However, due to measurement errors, WLS only provides globally minimized estimations. Therefore, some true values which are strictly within the operating limits might be estimated outside the boundaries. Thus, the objective function *J(x)* can be restricted with the equality constraints *c(x)* as:

$$\begin{aligned} \min \quad & J(x) = [z - h(x)]^T W [z - h(x)] \\ s.t. \quad & c(x) = 0 \end{aligned} \quad (16)$$

(16) can be solved by introducing Lagrangian relaxation:

$$L(x, \lambda) = J(x) - \lambda^T c(x) \quad (17)$$

Then, (17) can be derived to $\partial L/\partial x$=0, $\partial L/\partial \gamma = 0$.

III. Operating Limits of VSC

In practice, a VSC operates with two main limits, the converter voltage limit and the converter current limit. In general, the two limits can be critically set by adjusting the power injections. First, to express the converter voltage U_{ci} in terms of injected power P_{si} and Q_{si}, rewrite (5) as:

$$U_{ci} = U_{si} - I_{ci}(R_{ci} + jX_{ci}) \tag{18}$$

Then, substitute U_{ci} in (6) to represent I_{ci} as:

$$I_{ci} = [U_{si} - \frac{P_{si} - U_{si}^2 Y_i \sin\alpha_i}{Y_i U_{si}\sin(\delta_i - \alpha_i)}]/(R_{ci} + jX_{ci}) \tag{19}$$

Thus, U_{ci} can be written in terms of U_{si}:

$$U_{ci} = (P_{si} - U_{si}^2 Y_i \sin\alpha_i)/[U_{si} Y_i \sin(\delta_i - \alpha_i)] \tag{20}$$

substituting (20) to (7), the relationship between U_{si} and injected power P_{si}/Q_{si} is expressed as:

$$U_{si}^2 = \frac{Q_{si}\sin(\delta_i - \alpha_i) - P_{si}\cos(\delta_i - \alpha_i)}{Y_i \sin(\delta_i - 2\alpha_i)} \tag{21}$$

It should be noted that in (21), U_{si} can be completely described only by P_{si} and Q_{si}. Thus, it can be formulated with an abstract function, $U_{si} = f(P_{si}, Q_{si})$. Consequently, substitute $U_{si} = f(P_{si}, Q_{si})$ in (20), U_{ci} is expressed as:

$$U_{ci} = \frac{P_{si} - f^2(Q_{si}, P_{si}) Y_i \sin\alpha_i}{Y_i f(Q_{si}, P_{si}) \sin(\delta_i - \alpha_i)} \tag{25}$$

Therefore, the converter voltage can be controlled by adjusting the power injections. Furthermore, since the power injections are also restricted by the PWM factor, the boundaries of converter voltage can be preset. In general, the upper and lower limits, U_{ci}^{max} and U_{ci}^{min}, are preset at the operating point to avoid overmodulation. Similarly, the limit of converter current can also be deduced from the power injections as:

$$I_{ci}^* = S_{si}/U_{si} = (P_{si} + jQ_{si})/f(P_{si}, Q_{si}) \tag{26}$$

Obviously, the amplitude of converter current is limited within an operation circle in which the apparent power is maximized at the overmodulation point. To illustrate the limits and how the adjustment works, a toolbox, MatACDC [10] is utilized on a modified IEEE 5-bus system (shown in Fig. 2) to show the simulating results on two different cases. The preset power injections via VSC 1 are set at -60MW/-50MW and -130MW/-60MW, respectively. Meanwhile, the limits of voltage are set at 0.9 and 1.1 p.u., the maximum current is 1.2 p.u. Under these conditions, only VSC 1 violates the limits in two cases. Hence, the violations and adjustments of VSC 1 are depicted in Fig. 3.

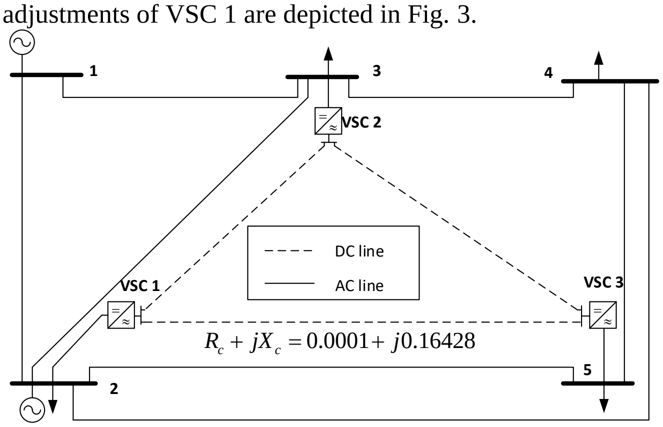

Figure 2. Modified IEEE 5-bus system with a three-terminal VSC link

As shown in Fig. 3, the operating range of VSC is restricted inside the shadow area, which is determined by two limits. Given the parameters in advance, we can predetermine the limits. Hence, no matter what the power injections are preset, the converter can self-adjust to ensure the outputs inside or on the boundaries. As depicted in Fig. 3(b) and (d), no actions are needed if the preset values do not violate the limits. However, for VSC 1, specific adjustments are required depending on the type of violations.

As shown in Fig. 3(a), the converter value with the power injections of -60MW/-50MW is 0.863 p.u., violating the lower voltage limit. Thus, the converter should reduce the reactive power injections along the y-axis until the voltage increases to 0.9 p.u. Hence, the real power is changed to -36.25MW to ensure the voltage limit. In the second case, as Fig. 3(c) depicts, the converter voltage is 0.893 p.u. and the current magnitude achieves 1.211 p.u., leading to the violations of two limits. Under this circumstance, both active and reactive power injections should be changed to the new operating values. Since controlling active power is the primary goal in VSC-MTDC system, the change of P_s should be small. Thus, the new operating power is changed to -121.21MW/8.96MW. Consequently, the adjusted converter current and voltage is 1.2 p.u. and 1.062 p.u. to ensure the safe operation.

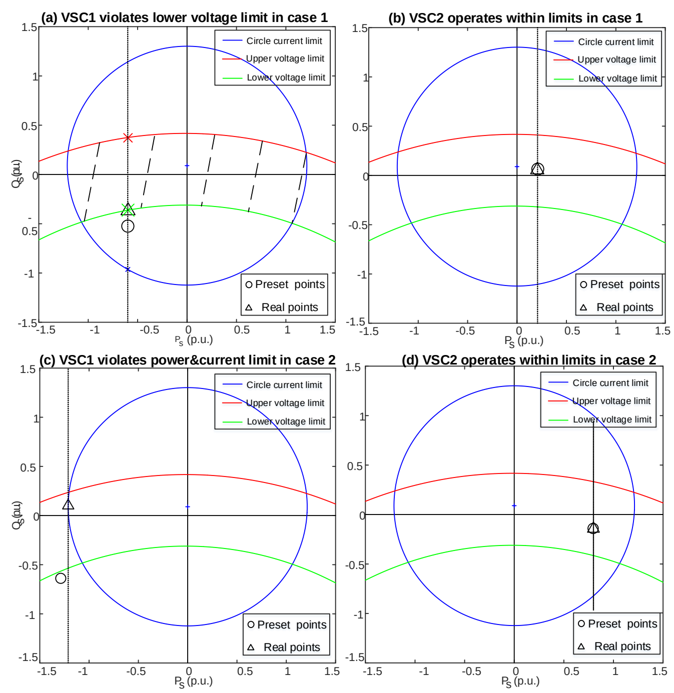

Figure 3. Converter limits and adjustments (a) voltage violation of VSC1 in case 1 (b) no violations of VSC 2 in case 1 (c) voltage & current violation of VSC1 in case 2 (d) no violations of VSC2 in case 2

Taking the operating limits into account, we need two additional steps. First, the operating ranges of all converters are pre-calculated based on the device parameters. Then, the SE results achieved from raw measurement data are checked by the ranges. Once the limits are violated, the corresponding adjusted values will replace the measurements and be formulated as equality constraints to modify WLS. Take VSC 1 in the first case for example, the WLS can be improved as:

$$\begin{cases} z = h(x) + e \\ c(x) = 0 \rightarrow \begin{cases} U_c - U_c^{\min} = 0 \\ Q_s - Q_s^{cal} = 0 \end{cases} \end{cases} \quad (27)$$

where Q_s^{cal} is calculated based on the minimum voltage.

IV. IMPROVED STATE ESTIMATION FOR VSC-MTDC

A. Measurements and state-variables

As shown in Fig. 1, the SE formulation can be generally represented by three parts:

$$z = \begin{bmatrix} z_{ac} \\ z_{ac-dc} \\ z_{dc} \end{bmatrix} = \begin{bmatrix} h_{ac}(x_{ac}, x_{ac-dc}, x_{dc}) \\ h_{ac-dc}(x_{ac}, x_{ac-dc}, x_{dc}) \\ h_{dc}(x_{ac}, x_{ac-dc}, x_{dc}) \end{bmatrix} + \begin{bmatrix} e_{ac} \\ e_{ac-dc} \\ e_{dc} \end{bmatrix} \quad (27)$$

Hence, the measurements and state variables can also be classified into three sets as listed in Table I.

TABLE I. DECOUPLED MEASUREMENTS AND STATE VARIABLES

Set	Measurements	State Variables
ac	$P_{acij}^m, Q_{acij}^m, P_{aci}^m, Q_{aci}^m, \lvert U_{aci}^m \rvert$	U_{aci}, θ_{aci}
dc	$P_{dcij}^m, P_{dci}^m, I_{dci}^m, U_{dci}^m$	U_{dci}
ac-dc	$P_{si}^m, Q_{si}^m, P_{ci}^m, Q_{ci}^m$ $\lvert U_{si}^m \rvert, \lvert U_{ci}^m \rvert, I_{ci}^m$	U_{ci}, M_i, δ_i

Meanwhile, the pseudo-measurements of the constant control values can be added to the measurement set without errors. Meanwhile, since the power injections from the converter to both AC and DC grids are codetermined by all the state variables. Therefore, the Sequential Method is very suitable to solve each part separately and update the common-coupling data sequentially until achieving global convergence.

B. Improved SE method with Lagrange relaxation

According to the previous discussions on the operating limits, the adjustments of power injections and WLS with equality constraint solved by Lagrange relaxation, an improved SE method for VSC-MTDC is proposed. The detailed flow chart is depicted in Fig. 4. The solution steps of the proposed method are given below:

Step 1: Read raw data from EMS.
Step 2-1: Classify the measurements, state variables and errors into three sets, *ac*, *dc* and *ac-dc*.
Step 2-2: Calculate the operating limits based on the preset operating points.
Step 3: Initialize state variables $[x_{ac}^0, x_{ac-dc}^0, x_{dc}^0]$. Set the iteration number *k=0.*
Step 4: Perform SE analysis for each part separately with WLS algorithm and get the inner estimations $U_{dc}^{e,k}$, $U_{ac}^{e,k}/\theta_{ac}^{e,k}$, $I_c^{e,k}/U_c^{e,k}/\delta^{e,k}$. (superscript *e* is for estimated results)
Step 5: Compute converter voltage $U_c^{cal,k}$ and converter current $I_c^{cal,k}$ based on the results from Step 4. $I_c^{cal,k} = (U_s^{e,k} - U_c^{e,k})/(R_c + jX_c)$, $U_c^{cal,k} = U_c^{e,k}$. (superscript *cal* is for calculated results)
Step 6: Do violations check, compare $U_c^{cal,k}$ and $I_c^{cal,k}$ with the operating limits calculated in Step 2-2. If violations happen, go to Step 7, otherwise, go to Step 9.
Step 7: Adjust power injections and add equality constraints to modify the WLS algorithm as $L^k(x,\lambda) = J^k(x) - \lambda^{T,k} c^k(x)$.
Step 8: Redo SE for the converter (*ac-dc*) with Lagrange relaxation.
Step 9: Check global convergence. If $\lvert P/Q_s^{cal,k} - P/Q_s^m \rvert \le \epsilon$ and $\lvert P/Q_c^{cal,k} - P/Q_c^m \rvert \le \epsilon$, go to Step 11, otherwise, go to Step 10.
Step 10: Set $k = k + 1$. Update the measurements of power injections and replace $P_s/Q_s/P_c/Q_c^m$ with $P_s/Q_s/P_c/Q_c^{cal,k}$. Then go to Step 4.
Step 11: Print final SE results.

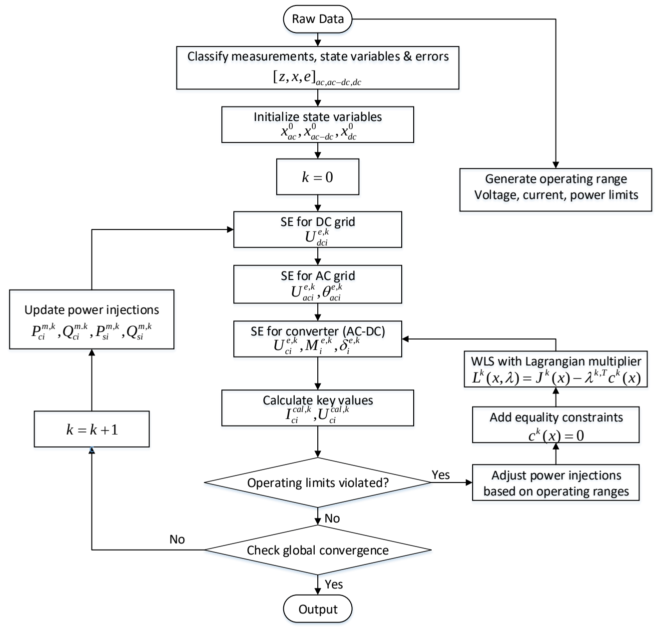

Figure 4. Flowchart of the improved SE method considering operating limits

Obviously, the overall calculation structure is the same as the traditional Sequential Method. Also, the major SE analysis is still based on WLS algorithm except for doing Lagrange relaxation.

V. SIMULATION RESULTS

Two VSC-MTDC systems, including the modified IEEE 5-bus system (C1) as shown in Fig. 2 and modified IEEE RTS-96 system (C2) in [11], are tested to illustrate the accuracy and efficiency of the proposed method. The SE data are simulated using the power flow results (true values) solved in MATLAB. Then, the corresponding measurement errors are modeled as Gaussian noise . The deviations are $\delta_{ac} = 0.04$, $\delta_{dc} = 0.02$ and $\delta_{ac-dc} = 0.03$.

Furthermore, to simulate the violations, the preset operating points of both systems are given in Table II. It should be noted that, with these preset points, the violations occur in both systems. In C1, the converter voltage of VSC 1 violates the lower limit boundary and the reactive power is adjusted to meet the requirement. In C2, both the voltage and current of VSC 3 are violated, leading to the adjustments of active and reactive power injections. Under this circumstance, the SE results of the proposed method (PM) are compared with the true values (TR) and the estimations of the conventional method (CO), in Table III.

TABLE II. PRESET OPERATING POINTS OF TEST SYSTEMS

Constant input		P_s (MW)	Q_s (MW)
C1	VSC 1	-60	-50
	VSC 2(slack)	0	0
	VSC 3	35	5
C2	VSC 1(slack)	0	50
	VSC 2	75.3	-50
	VSC 3	-141.9	130
	VSC 4(slack)	131.5	75.9
	VSC 5	-61.7	0
	VSC 6	-123.4	-10
	VSC 7	50	20

TABLE III. COMPARISONS OF THE SE RESULTS AND TRUE VALUES

Values		U_{dc} (p.u.)	U_c (p.u.)	M	σ	P_s (MW)	Q_s (MW)
C1							
VS C1	TR	1.008	**0.900**	0.7919	10.516	-60.00	**-36.25**
	PM	1.008	**0.900**	0.7919	10.523	-59.98	**-36.25**
	CO	1.007	**0.893**	0.7918	10.543	-59.54	**-36.83**
VS C2	TR	1.000	1.007	0.7022	-3.243	20.77	7.13
	PM	1.000	1.007	0.7022	-3.233	20.75	7.15
	CO	1.000	1.006	0.7022	-3.227	20.81	7.14
VS C3	TR	0.998	0.995	0.7087	-5.591	35.00	5.00
	PM	0.997	0.995	0.7085	-5.595	34.97	4.98
	CO	0.997	0.994	0.7092	-5.596	34.96	4.99
C2							
VS C1	TR	1.000	1.192	0.5930	-17.386	141.44	50
	PM	1.000	1.193	0.5929	-17.375	141.38	49.97
	CO	1.000	1.190	0.5937	-17.381	141.37	49.98
VS C2	TR	1.012	0.953	0.7511	-11.807	75.3	-20.85
	PM	1.013	0.953	0.7513	-11.822	75.19	-20.94
	CO	1.013	0.953	0.7513	-11.821	75.21	-20.95
VS C3	TR	1.025	**1.088**	0.6662	15.252	**-231.52**	**4.97**
	PM	1.025	**1.088**	0.662	15.248	**-231.52**	**4.97**
	CO	1.024	**1.101**	0.658	15.357	**-232.77**	**5.13**
VS C4	TR	1.000	1.128	0.6266	-7.988	123.38	75.90
	PM	1.000	1.127	0.6269	-7.972	123.41	75.42
	CO	1.000	1.127	0.6269	-7.981	123.50	75.67
VS C5	TR	1.017	1.060	0.6785	8.284	-61.70	0
	PM	1.016	1.058	0.6791	8.310	-61.77	0.01
	CO	1.015	1.057	0.6790	8.305	-61.95	0.02
VS C6	TR	1.019	1.026	0.7026	8.874	-123.40	0
	PM	1.019	1.025	0.7029	8.865	-122.92	-0.01
	CO	1.019	1.024	0.7032	8.854	-122.85	0.01
VS C7	TR	1.011	1.098	0.6511	-6.524	50.00	20.00
	PM	1.012	1.102	0.6503	-6.487	49.87	19.95
	CO	1.011	1.095	0.6524	-6.511	49.83	19.88

To begin with, it is obvious that for the VSCs operating within limits, both the improved and conventional SE methods can provide accurate estimations (compared with the true values). The reason is that by doing WLS algorithms sequentially, the measurement errors in the converters can be eliminated from both AC and DC sides. However, the results are very different for the converters (VSC 1 of C1 and VSC 3 of C2) that have changed operating points due to the violations. In C1, the reactive power injection of VSC 1 is fixed on -36.25MW by modulating PWM to ensure that the converter voltage is 0.900 p.u. The improved method detects the violation and modify WLS by adding two equations for equality constraints. Therefore, the corresponding estimated results can reflect the true values. Similarly, in C2, both active and reactive power injections on VSC 3 are changed to -231.52MW and 4.97MW to avoid the violations. Also, we added the equality constraints to obtain accurate results. The conventional method, however, can't deal with this situation.

VI. CONCLUSION

In this paper, an improved state estimation method is proposed for VSC-MTDC system with the consideration of operating limits. By transforming the converter voltage and converter current in terms of the power injections, the operating limits of VSC are presented. Thus, the fast adjustments of PWM is adopted in the steady-state model. The conventional Sequential Method is modified so that the SE method detects the violations and give accurate estimated results. First, a procedure of violations check is implemented to monitor the estimated results calculated from each decoupled grid. Then, once the violations occur, the corresponding equality constraints are added to the WLS equations, and subsequently solved by using Lagrange relaxation. Thus, the improved method obtains the accurate operating values which are the same as the boundary limits. The test results of two systems verify the accuracy and efficiency of the proposed method.

REFERENCES

[1] Y. Xue, X. Zhang and C. Yang, "AC Filterless Flexible LCC HVDC With Reduced Voltage Rating of Controllable Capacitors," *IEEE Trans. Power Systems*, vol. 33, no. 5, pp. 5507-5518, Sept. 2018.

[2] W. Feng, et al., "Using virtual buses and optimal multipliers to converge the sequential AC/DC power flow under high load cases," *Electric Power Systems Research*, vol. 177, Sep. 2019

[3] D. Shu, X. Xie, H. Rao, X. Gao, Q. Jiang and Y. Huang, "Sub- and Super-Synchronous Interactions Between STATCOMs and Weak AC/DC Transmissions with Series Compensations," *IEEE Trans. Power Electronics*, vol. 33, no. 9, pp. 7424-7437, Sept. 2018.

[4] F. Chen, et al., "Reliability assessment method of composite power system with wind farms and its application in capacity credit evaluation of wind farms," *Electric Power System Research*, vol. 166, pp.73-82, Jan 2019.

[5] A. K. Sinha, L. Roy and H. N. P. Srivastava, "A decoupled second order state estimator for AC-DC power systems," *IEEE Trans. Power Syst.*, vol. 9, no. 3, pp. 1485-1493, Aug. 1994.

[6] M. Z. Haque and A. Kalam, "AC/Multiterminal DC Power System State Estimation-A Sequential Approach," *Electric Machines & Electromechanics*, vol. 12, no. 1, pp. 27-42, 1987

[7] Q. Ding, T. S. Chung and B. Zhang, "An improved sequential method for AC/MTDC power system state estimation," *IEEE Trans. Power Syst.*, vol. 16, no. 3, pp. 506-512, Aug. 2001.

[8] A. de la Villa Jaen, E. Acha and A. G. Exposito, "Voltage Source Converter Modeling for Power System State Estimation: STATCOM and VSC-HVDC," *IEEE Trans. Power Syst.*, vol. 23, no. 4, pp. 1552-1559, Nov. 2008.

[9] V. Donde, X. Feng, I. Segerqvist and M. Callavik, "Distributed State Estimation of Hybrid AC/HVDC Grids by Network Decomposition," *IEEE Trans. on Smart Grid*, vol. 7, no. 2, pp. 974-981, March 2016.

[10] J. Beerte, MatACDC Toolbox, The University of Leuven, 2012. Available on https://www.esat.kuleuven.be/electa/teaching/matacdc.

[11] J. Beerten, S. Cole and R. Belmans, "Generalized Steady-State VSC MTDC Model for Sequential AC/DC Power Flow Algorithms," *IEEE Trans. Power Syst.*, vol. 27, no. 2, pp. 821-829, May 2012.